Numerical Simulation of Double-Droplet Continuously Impact on Cold Surface with Different Wettability

*HU Anjie**, *YUAN Qiaowei*, *GUO Kaiyue*, *LIU Dong*

School of Civil Engineering and Architecture, Southwest University of Science and Technology, Mianyang 621010, P.R. China

(Received 31 March 2023; revised 10 August 2023; accepted 15 October 2023)

Abstract: The numerical simulation method combining solidification/melting model and volume of fluid (VOF) model is used to study the freezing behavior of double-droplet continuously impacting cold surfaces with varying wettability under low-velocity conditions. The droplet spreading and phase transition processes under two contact modes (diffusion contact and contraction contact) are compared. The simulation results indicate that the coalescence of droplets has a significant impact on their morphology. When two droplets continuously impact the hydrophilic surface, the maximum spreading factor of diffusion contact increases by 26%—38% compared with that of a single droplet impact, and the maximum spreading factor of contraction contact increases by 15%—30% compared with that of a single droplet impact. On superhydrophobic surfaces, the maximum spreading coefficient difference between single and double-droplet impacts is less than 2%, which can be ignored. In addition, an analysis is conducted on the collision between double droplets and superhydrophobic surfaces at low temperatures, and the impact patterns of complete rebound, partial rebound, and full adhesion on droplet aggregation and solidification processes under different contact modes are obtained.

Key words: double-droplet; freezing behavior; solidification/melting model; VOF model; superhydrophobic surface

CLC number: V211.1 **Document code:** A **Article ID:** 1005-1120(2023)06-0714-13

0 Introduction

When an aircraft flying at a high altitude passes through the cumulonimbus cloud layer in a low-temperature environment, the supercooled droplets impact the surface of the aircraft and freeze, which will affect the dynamics of the aircraft and cause the aircraft to crash. Due to the great threat of icing to aircraft safety, numerous anti-icing methods have been proposed. Taking inspiration from nature's "lotus leaf effect", scientists have developed a bionic surface with superhydrophobic properties, exhibiting both low adhesion and effective self-cleaning capabilities[1]. In the study conducted by Liu et al.[2], experimental methods were employed to examine droplet impact on surfaces with varying wettability. Their findings suggested that droplet impact on superhydrophobic surfaces exhibited remarkable hydrophobic characteristics. On the other hand, Sun et al.[3] used numerical simulations to examine the morphological evolution of droplets impacting superhydrophobic surfaces. They identified four distinct stages during the process: Falling, spreading, contracting, and rebounding. Previous studies have demonstrated that superhydrophobic surfaces effectively reduce the contact time between droplets and the surface, facilitating droplet rebound and making them suitable for deicing applications. However, further research is needed to fully comprehend the mechanism of droplet icing on superhydrophobic surfaces.

In recent years, there have been experimental and numerical investigations conducted on the mechanisms and phenomena of droplet icing on cold sur-

*Corresponding author, E-mail address: anjie@swust.edu.cn.

How to cite this article: HU Anjie, YUAN Qiaowei, GUO Kaiyue, et al. Numerical simulation of double-droplet continuously impact on cold surface with different wettability[J]. Transactions of Nanjing University of Aeronautics and Astronautics, 2023, 40(6): 714-726.

http://dx.doi.org/10.16356/j.1005-1120.2023.06.008

faces, including both static and impact-freezing features. Recent years have witnessed both experimental and numerical investigations focusing on the mechanisms and phenomena of droplet icing on cold surfaces, encompassing static and impact-freezing features. Yang et al.[4] conducted a visual experiment to examine the icing behavior of supercooled droplets impacting a cylindrical surface. The study emphasized the significance of temperature as crucial factors affecting droplet solidification. Furthermore, previous research has suggested that enhancing the contact area can lead to higher nucleation rates, lower critical adhesion temperatures, and shorter freezing durations for droplets[5-7]. However, it is challenging to depict the movement of the phase shift within the droplet due to experimental constraints. To tackle this concern, researchers have utilized computational models as a supplementary method to explore the freezing characteristics of droplets in addition to experimental data. In this regard, Blake et al.[8] introduced a technique that combines the volume of fluid (VOF) coupled level-set method to track the air-water interface and the enthalpy porous approach to model the liquid-solid interface, effectively simulating the impact and solidification of supercooled water droplets on a cold surface. Expanding on this, Chang et al.[9] employed the same method to address the solidification problem, conducting a comprehensive analysis of the temporal evolution of various thermophysical properties of the droplet. In a separate study, Zhang et al.[10] conducted experiments and simulations to explore the behavior of droplets impacting a cold surface. Their research effectively combined the VOF model with the solidification/melting phase transition model, yielding results that closely matched the experimental observations.

These research revealed the deep mechanism of the droplet icing process. Nonetheless, most studies have focused on individual droplets, which might not provide an accurate representation of real icing conditions. This is because multiple droplets can coalesce upon impact, forming larger droplets. The interaction and intense contact between neighboring droplets during the spreading and solidification process introduce highly intricate impact dynamics, which fundamentally differ from impacts involving a single droplet. Therefore, understanding the behavior of multiple-droplet impacts is essential for comprehensive icing analysis[11-13]. In their investigation, Gao et al.[14] conducted a study on the dynamic behavior of multiple droplets, analyzing the rebound dynamics of double droplets impacting an inclined superhydrophobic surface. The research unveiled a significant correlation between droplet springback behavior and droplet spacing. Likewise, Wang et al.[15] investigated the rebound dynamics of double droplets on a superhydrophobic surface, identifying rebound modes based on the center spacing and inclination angle between the droplets.

However, the majority of droplet-icing research has been focused on single droplet impact icing. Multi-droplet impact icing is more commonly observed in practical scenarios, yet only a limited number of study have explored this phenomenon[16-17]. This study aimed to investigate the dynamics and ice formation characteristics of double droplets impacting a solid surface through numerical simulation. For this purpose, the commercial computational fluid dynamics (CFD) software ANSYS Fluent[18] was utilized. The VOF model[19] was utilized to simulate the behavior of droplets, while the enthalpy-porosity model was adopted to study the solidification process of the droplets. The study specifically focused on examining the impact of the contact angle on the solidification process during both spreading and contracting phases. By tracking the spreading factor and morphological changes over time during the impact-freezing process, valuable insights were obtained into the polymerization and freezing characteristics of the double droplet when it impacts a cold surface.

1 Numerical Model

1.1 Multiphase model

In this study, the VOF model, originally proposed by Hirt and Nichols[19] based on the Eulerian method, is utilized. This model effectively tracks

the interface between the gas and liquid phases, enabling accurate calculation of the fluid distribution in each computational cell within this framework.

$$\alpha_j = \frac{\text{volume of the } j\text{th phase}}{\text{cell volume}} \tag{1}$$

where $\sum \alpha_j = 1$. In this simulation, a two-phase flow model is utilized, treating the mixture of water and ice, along with liquid water, as a single liquid phase, while considering air as the second phase. In this model, the mass transition equation is represented as

$$\frac{\partial}{\partial t}(\alpha_j \rho_j) + \nabla(\alpha_j \rho_j \boldsymbol{u}) = 0 \quad j = 1,2 \tag{2}$$

where ρ_j is the density of the jth phase, and $\boldsymbol{u}$ the velocity of the fluid.

The conservation of momentum is extended to encompass the entire computational domain by considering a single grid element.

$$\frac{\partial}{\partial t}(\rho \boldsymbol{u}) + \nabla(\rho \boldsymbol{u}\boldsymbol{u}) = -\nabla p + \nabla\mu(\nabla \boldsymbol{u} + (\nabla \boldsymbol{u})^{\mathrm{T}}) + \rho \boldsymbol{g} + \boldsymbol{F}_{\mathrm{st}} + \boldsymbol{S}_{\mathrm{M}} \tag{3}$$

where the total fluid density ρ and the average viscosity μ in each cell are as follows

$$\rho = (\alpha_j \rho_j) \quad \mu = \sum\nolimits_j (\alpha_j \mu_j) \quad j = 1,2 \tag{4}$$

The gas-liquid interface is influenced by the volume surface tension $\boldsymbol{F}_{\mathrm{st}}$. Additionally, the freezing process is taken into account through the momentum source term $\boldsymbol{S}_{\mathrm{M}}$. To compute the surface tension force, we employ the continuum surface force (CSF) model proposed by Brackbill et al.[20] in this study

$$\boldsymbol{F}_{\mathrm{st}} = \sigma \frac{\rho \kappa \nabla \alpha}{0.5(\rho_1 + \rho_2)} \tag{5}$$

where the surface tension coefficient σ and the interface curvature κ are related as

$$\kappa = \nabla \cdot \frac{\nabla \alpha}{|\nabla \alpha|}\bigg|_{\alpha = 0.5} \tag{6}$$

The determination of the contact angle at the wall involved an assessment of the free interfacial normal vector in the control body at the wall, influencing the interfacial curvature and the source terms related to surface tension. The mathematical expression for the normal vector is

$$\boldsymbol{n} = \boldsymbol{n}_{\mathrm{w}} \cos\theta_{\mathrm{w}} + \boldsymbol{t}_{\mathrm{w}} \sin\theta_{\mathrm{w}} \tag{7}$$

where $\boldsymbol{n}_{\mathrm{w}}$ is the unit vector normal, tangential to the wall $\boldsymbol{t}_{\mathrm{w}}$, and θ_{w} the prescribed contact angle.

1.2 Solidification/melting model

On the cold surface, droplets undergo a process of solidification, which consists of five distinct stages: Droplet impact, nucleation, recalescence, and solid cooling. To account for the complexities and uncertainties in predicting nucleation delay, this study assumes nucleation occurs upon droplet impact with the cold surface. Moreover, the recalescence process is considered to be much faster than the evolution of the contact line, as this commonly adopted in previous studies.

The enthalpy-porosity phase change model is utilized in this study to simulate the solidification-melting process within the double droplet[14]. Notably, the recalescence phase is neglected in this model, and the energy equation governing the process is

$$\frac{\partial}{\partial t}(\rho h) + \nabla(\rho \boldsymbol{u} h) = \nabla(\lambda \nabla T) \tag{8}$$

where λ represents the thermal conductivity, and the enthalpy value h is defined as the combined sum of latent enthalpy h_{le} and sensible enthalpy h_{se}, shown as

$$h = h_{\mathrm{se}} + h_{\mathrm{le}} \tag{9}$$

where the sensible enthalpy h_{se} is mathematically expressed as

$$h_{\mathrm{se}} = h_{\mathrm{ref}} + \int_{T_{\mathrm{ref}}}^{T} C_p \, \mathrm{d}T \tag{10}$$

where the reference enthalpy h_{ref}, the reference temperature T_{ref}, and the thermal capacity C_p are important parameters in the simulation. The latent enthalpy during the solidification/melting process is governed by the liquid water fraction present in the droplet, shown as

$$h_{\mathrm{ls}} = L\gamma \tag{11}$$

where L is the latent heat and γ the liquid water fractionand. Tare relevant parameters in the model. The liquid water fraction is assumed to be a function of temperature

$$\gamma = \begin{cases} 0 & T < T_{\mathrm{solid}} \\ \dfrac{T - T_{\mathrm{solid}}}{T_{\mathrm{liquid}} - T_{\mathrm{solid}}} & T_{\mathrm{solid}} \leqslant T \leqslant T_{\mathrm{liquid}} \\ 1 & T > T_{\mathrm{liquid}} \end{cases} \tag{12}$$

where the critical temperatures T_{solid} and T_{liquid} are defined as the temperatures at which complete solidification and melting of the droplet occur, respectively. To preserve the shape of the ice-water interface, a small interval of $[T_{solid}, T_{liquid}]$ is always set in the model.

In previous studies, the enthalpy-porosity method has been consistently utilized to simulate the ice-water mixing area. This method treats the ice-water mixing area as a porous region, and the momentum source term $\boldsymbol{S}_M$ in Eq.(3) is expressed as

$$\boldsymbol{S}_M = \frac{(1-\gamma)^2}{\gamma^3+\varepsilon} C_{mush}\boldsymbol{u} \tag{13}$$

where ε is the introduced as a small value ($\varepsilon = 0.001$) to prevent a zero denominator; C_{mush} is related to the shape of the porous medium and the viscosity coefficient. Previous studies have commonly used values between 10^{-4} and 10^{-7}.

1.3 Numerical model validation

In this study, we utilize the proposed model to examine the continuous impact of double droplets on surfaces with varying wettability under cold conditions. To optimize computational resources, a two-dimensional rectangular domain measuring 12.5 mm×10.0 mm in length and width is utilized. At the domain's edge, a rotational axisymmetric boundary condition is established, as illustrated in Fig.1. For this study, the bottom wall is subjected to a non-slip boundary condition, and other boundaries are designated as pressure outlet boundaries. Both droplets have a diameter D_0=2.5 mm, and their initial velocity V_0 is set to 0.5 m/s. The space S between the droplets is set at 3.0 and 3.5 mm. The direction of the gravitational force is set aligned with the impact direction. In this work, a mesh with square cells, generated using the structured method, is adopted since it better captures the interface of the droplets through the VOF model. To enhance mesh resolution and save computational resources, refinement is implemented near the wall and impact axis. Four grid sizes (60, 30, 15, 7.5 μm) are adopted to verify the grid independence of the model. The simulation evolutions of spreading factor (defined as the ratio of the spreading diameter of the drop on the surface D and the initial diameter of the droplet D_0, as shown in Fig.2) of single droplet impact with different grid sizes are compared. The simulation phase settings align with those in Ref.[10]. Maintaining model stability, a global Courant number of 0.2 is imposed. The grid size verification results are shown in Fig.3. As seen in Fig.3, simulation results with grid sizes of 15 and 7.5 μm are notably similar. Consequently, to improve computational efficiency, the grid size of 15 μm is adopted in this study. The final calculation area comprises 216 233 square grids.

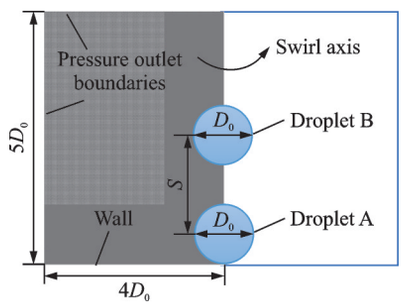

Fig.1 Schematic diagram of physical model and mesh

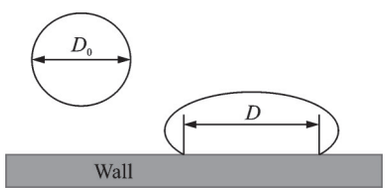

Fig.2 Schematic diagram of droplet shape parameters

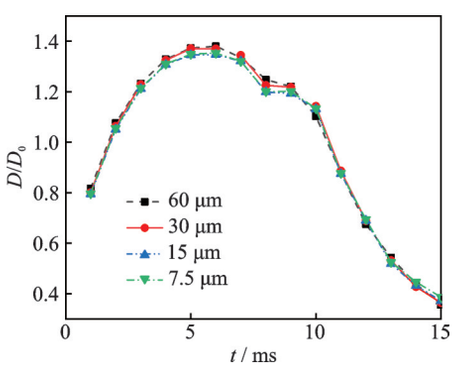

Fig.3 Grid independence verification

1.4 Validation of numerical model

This study validates the performance of the solidification/melting model by comparing it with data from Refs.[10, 21-22]. Figs.4(a, b) illustrate the morphological progression of droplets after impacting a cold surface, using experimental photographs

and two-dimensional numerical simulation results. The specific experimental parameters include: D_0= 2.84 mm, T_a= −5 ℃, T_0=0.1 ℃, T_s= −30 ℃, V_0=0.7 m/s, θ_s=160°, with droplets' physical parameters align with those in Ref.[10]. The comparison between the simulation data obtained from the coupled VOF model and Zhang's experimental results is illustrated in Fig.4(c). The observed good agreement between the simulation and experimental data demonstrates the accuracy of the coupled model in predicting the behavior and freezing characteristics of droplets upon impact with cold surface.

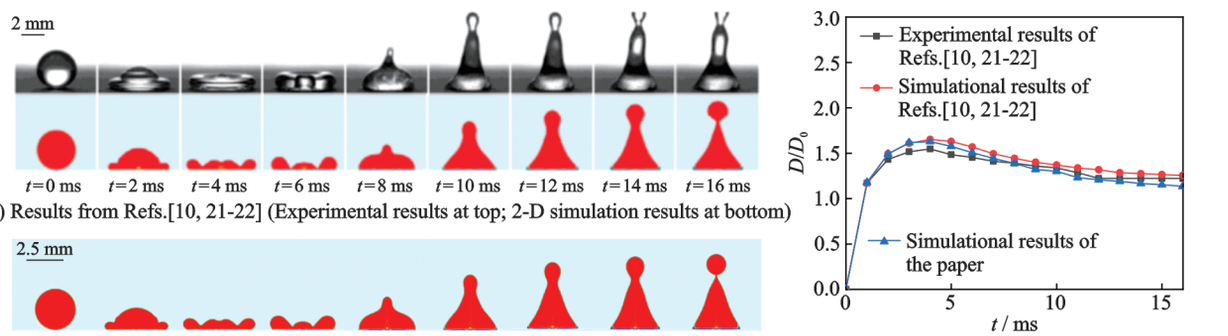

(a) Results from Refs.[10, 21-22] (Experimental results at top; 2-D simulation results at bottom)

(b) Simulation results for two-dimensional axisymmetric swirl model

(c) Comparison of spreading factor D/D_0 over time

Fig.4 Comparison of simulation and experimental results of droplets impacting on superhydrophobic cold surface (T_a= −5 ℃, T_s= −30 ℃)

2 Results and Discussion

The focus of this paper is to investigate the impact-icing phenomena resulting from double droplets colliding on cold surfaces featuring varying wettability. The study is conducted using a two-dimensional rotational axisymmetric model to investigate the process under three different contact angles θ_s and temperatures. Table 1 presents the cases for each parameter, with the spacing S between double droplet set is at either 3.0 mm or 3.5 mm. The evolution of the morphology, the infiltration and spreading factors, and the variation characteristics of the velocity and temperature distributions during droplet impact under different conditions are obtained through simulation. In Table 1, D_{0A}, D_{0B} are the initial diameters of droplets A, B; V_{0A}, V_{0B} the initial velocities of droplets A, B; and T_0, T_a, T_s the initial temperatures of the droplets, air and solid surface.

Table 1 Simulation parameter combinations

θ_s/(°)	S/mm	D_{0A},D_{0B}/mm	V_{0A},V_{0B}/(m·s^{-1})	T_0,T_a, T_s/℃	T_0,T_a, T_s/℃	T_0,T_a, T_s/℃
160	3.5	2.5,2.5	0.5,0.5	15,15, 15	15,15, −30	0.1,−5, −30
	3.0	2.5,2.5	0.5,0.5			
	Single	2.5	0.5			
100	3.5	2.5,2.5	0.5,0.5	15,15, 15	15,15, −30	0.1,−5, −30
	3.0	2.5,2.5	0.5,0.5			
	Single	2.5	0.5			
40	3.5	2.5,2.5	0.5,0.5	15,15, 15	15,15, −30	0.1,−5, −30
	3.0	2.5,2.5	0.5,0.5			
	Single	2.5	0.5			

2.1 Morphology evolution of droplets

The changes in droplet shape and morphology upon impact are depicted in Fig.5 and Fig.6, which show the dynamic evolution of double-droplet interacting with a hydrophilic surface at various temperatures. When droplets at room temperature T_a=15 ℃ collide with a surface at the same temperature T_s= 15 ℃, the initial distance between the droplets does not have a significant impact on the kinetic behavior of the droplets under conditions without phase changing. After impacting the surface, the droplets disperse extensively, resulting in the formation of a thin layer of water that remains on the surface. The residual kinetic energy is minimal, leading to gradual droplet contraction and uniform kinetic characteristics of the dual droplet at two distinct contact distances of 3.0 mm and 3.5 mm. At this juncture, the primary factors contributing to energy dissipation involve the friction between the droplets and the hy-

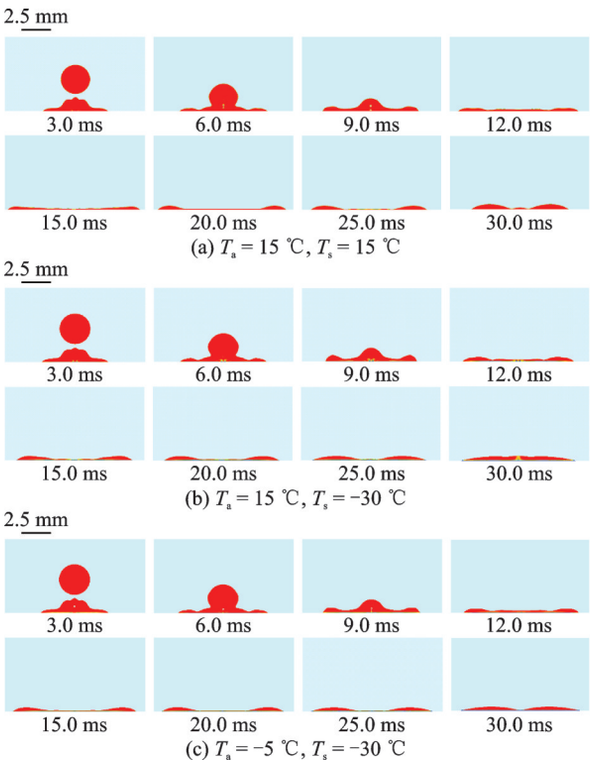

Fig.5 Morphologies of double-droplet continuously impacting hydrophilic surface of S = 3.0 mm

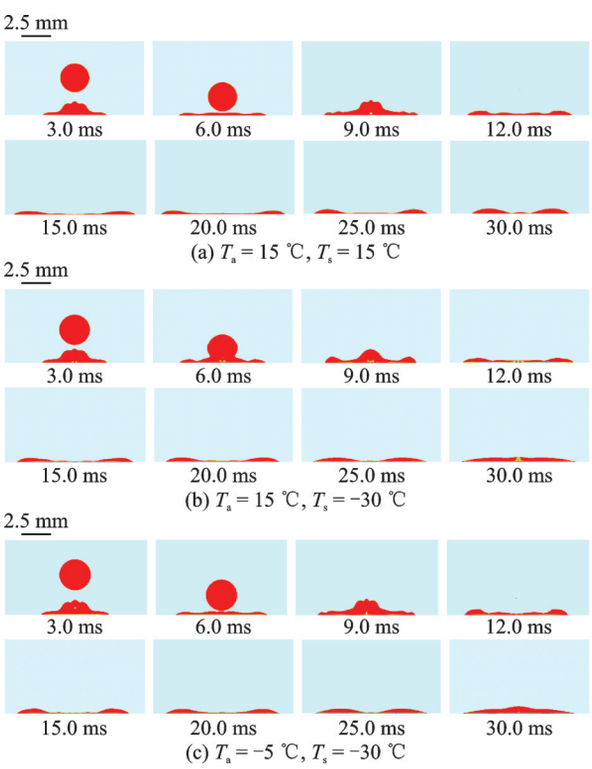

Fig.6 Morphologies of double-droplet continuously impacting hydrophilic surface of S = 3.5 mm

drophilic surface, as well as the disruption of contact during the interaction between the double droplets. Upon impact on cold surfaces T_s = −30 ℃, the thermal exchange between the underlying fluid and the cold surface hinders the spreading characteristics of the droplets. As a result, a slender layer of ice is formed, and the droplets adhere to the cold surface. Consequently, the diffusion of droplets maintains a nearly constant spreading diameter throughout the process of shrinkage. The findings indicate that the morphological evolution of droplets after contact is not significantly influenced by the initial distance between droplets and their initial temperature, in the case of hydrophilic cold surfaces.

Under different contact moments and temperature conditions, Fig.7 and Fig.8 illustrate the evolutions of droplet morphology resulting from the impact of double-droplet on hydrophobic and superhydrophobic surfaces. The space between the two droplets has a significant impact on their kinetic properties. Specifically, when the initial space is 3.0 mm, the first droplet is still undergoing spreading when it comes into contact with the second droplet. This phenomenon is referred to as the spreading contact in this study, when the interelectrode distance is 3.5 mm, the initial droplet has sufficient time to reach its maximum spread and subsequently begins to retract. The second droplet comes into contact with the first droplet during the contraction stage, which corresponds to the contraction contact in this study.

According to the morphology of double-droplet continuously impacting on the hydrophobic surface, it can be found that, in the case of a surface at normal temperature, the contact line contracts after reaching the maximum, and then vibrates on the wall. In the case of cold surface (T_s = −30 ℃), a layer of ice develops at the interface between the droplet and the wall, resulting in the droplet adhering to the surface. The droplet's receding process does not exhibit significant changes, and during the receding of the first droplet, air tends to be trapped inside the droplet when the second droplet impacts the surface. This generates small droplets and fluctuations on the edge of the droplet, the research findings indicate that the icing process has a significant

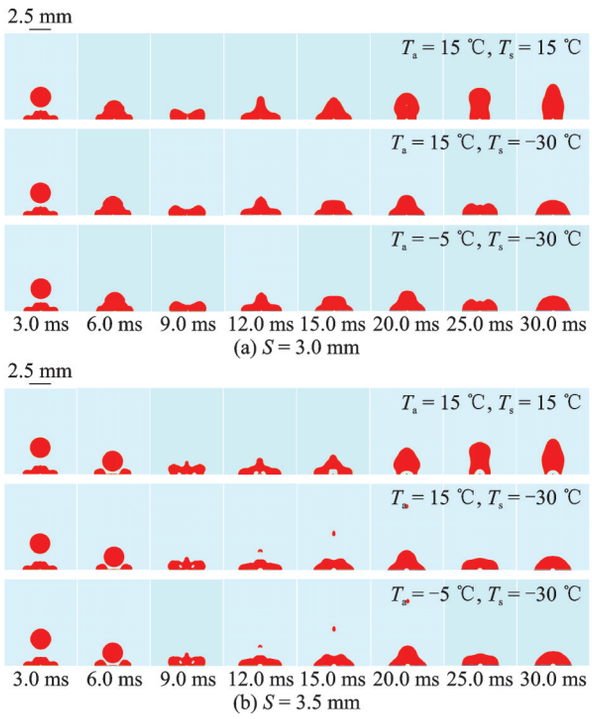

Fig.7 Morphologies of double-droplet continuously impacting hydrophobic surface

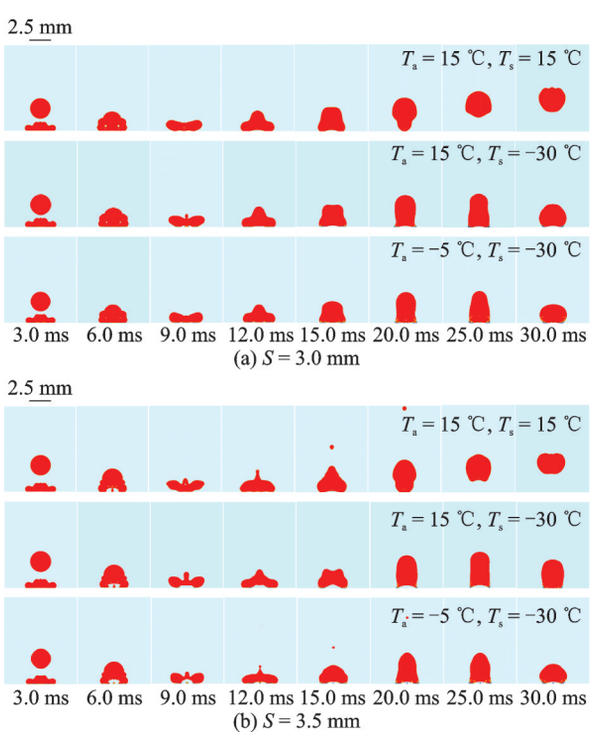

Fig.8 Morphologies of double-droplet continuously impacting superhydrophobic surface

impact on the behavior of droplets on the surface. However, the initial spacing between droplets has a relatively minor effect.

Compared to Fig.7, the adhesion and viscous dissipation of superhydrophobic surfaces shown in Fig.8 are reduced, and the droplets have enough energy to bounce back after merge into the large droplet. The initial spacing of droplets has a reduced impact during this time period. When the temperature of the superhydrophobic surface is low (T_s = −30 ℃), the air pocket formed during the contraction contact impact is more pronounced compared to hydrophobic surfaces. Additionally, the interface experiences vibration during the combination of these double droplets.

Based on the data regarding the evolution of double-droplet shapes across various surfaces and environmental temperatures, it is evident that the primary factors impacting droplet behavior are the surface's wettability and temperature. While the influence of the impact moment of the secondary droplet is much smaller.

2.2 Spreading factor evolution during impact

Figs.9—11 illustrate the progression of the spreading factor to better assess the influence of initial contact moment and temperature conditions on the droplet freezing process. The spreading factor β of the double droplet is given by the ratio between the wetting diameter of the droplet on the solid surface and the diameter of a single droplet, shown as

$$\beta = \frac{D_{wet}}{D_0} \tag{14}$$

where D_{wet} and D_0 are the wetting contact line and the initial diameter of a droplet.

As shown in Fig.9, the spreading factors that arise from double-droplet impacts are greater than those observed with single droplet when the droplet collides on the hydrophilic surface. This phenomenon is notably apparent in the absence of phase transition conditions, where the maximum spreading factor rises by 38% and 30% for spreading and contraction contacts, respectively. When considering cold surfaces, the temperature of the droplet at the beginning and the distance between adjacent droplets in contact have minimal impact on the maximum spreading factor. Specifically, there is an increase of 26% and 15% for spreading contact and contraction contact, respectively.

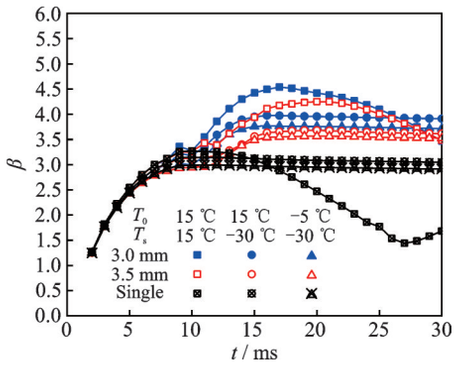

Fig.9 Evolution of spreading factor of double-droplet continuously impacting hydrophilic surface with different temperatures

Fig.10 shows the impact of the double-droplet on the maximum spreading factor on hydrophobic surfaces, revealing a significant reduction. At room temperature, the maximum spreading factor increases by 3% for spreading contacts and 0.2% for contraction contacts compared to the impact of a single droplet. With a cold surface, the maximum spreading factor experiences an increase of 8% and 13% for spreading and contraction contacts, respectively. These findings demonstrate that the impact of double droplets diminishes as the surface contact angle rises.

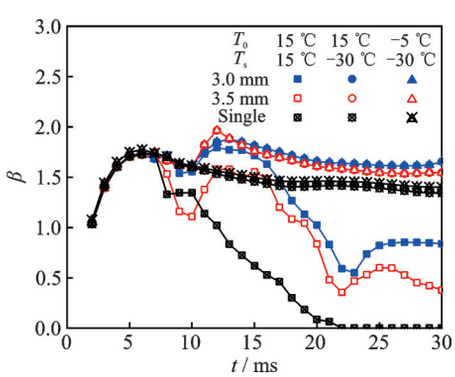

Fig.10 Evolution of spreading factor of double-droplet continuously impacting hydrophobic surface with different temperatures

Upon achieving superhydrophobicity, the impact of two droplets on the superhydrophobic surface yields a maximum spreading factor that closely resembles that produced by a single droplet, with a maximum deviation of approximately 2%, even at varying initial temperatures. This suggests that an increased contact angle can mitigate the impact of secondary droplets. In the case of cold superhydrophobic surfaces, the spreading factor is notably influenced by both the spacing between droplets and the initial temperature of the droplets. The merging process results in the droplet enclosing numerous voids, which consequently reduces the contact area with the frigid surface. Additionally, owing to the hydrophobic characteristics of the superhydrophobic surface, the droplet tends to undergo a shock process upon impact. During this process, the droplet polymerizes and entraps a minute quantity of air. Due to the comparatively lower initial temperature of the supercooled droplet, the supercooled droplet undergoes a faster freezing process upon collision with the cold surface. Furthermore, the presence of an ice layer at the bottom of the droplet significantly impacts the merging process of the droplets.

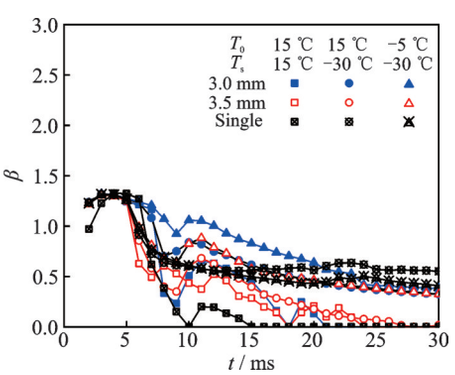

Fig.11 Evolution of spreading factor of double-droplet continuously impacting superhydrophobic surface with different temperatures

2.3 Heat transfer and solidification characteristics

To analyze the heat transfer and phase transition that occur during the impact of two droplets on the surface, this section presents and discusses the icing, temperature, and velocity evolutions.

Fig.12 illustrates the cloud diagram representing the phase transition of icing during a double-droplet continuously colliding with a superhydrophobic low-temperature surface. Ice nucleation occurs at the interface of the contact line between the initial droplet and the chilled surface, and the ice layer thickness gradually increases as the droplet cools due to the low surface temperature. After the sec-

ondary droplet hits and the contact line expands (t= 10 ms), a slender layer of a mixture of water and ice (yellow and red phases) develops in the vicinity of the droplet's outer contact region. During the contraction phase, due to the insufficient viscosity of the water-ice mixture, the droplet ruptures the thin ice layer upon contact with the polymerization. As a result, a larger air pocket forms at the bottom of the polymerized droplet, causing the contact area at the bottom to adopt a more circular shape.

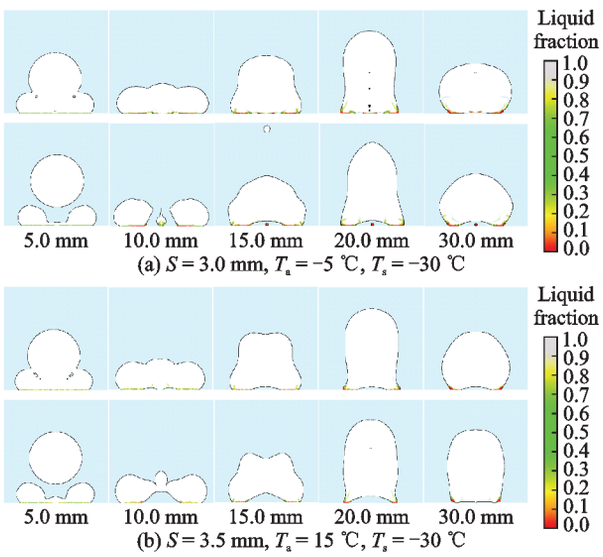

Fig.12 Icing phase transition of double-droplet continuously impacting superhydrophobic cold surface

Fig.13 displays the velocity and temperature distributions that correspond to the data presented. Based on the velocity distributions depicted in Fig.13, it can be observed that the droplet's velocity is at its maximum during the initial stage of contact. The magnitude of velocity decreases following the impact as a result of viscous dissipation induced by the droplet's impaction. At the base of the droplet, the velocity tends towards zero as ice crystallizes on the solid substrate. The zero-velocity zone expands proportionally to the thickness of the ice layer. The temperature distribution in Fig.13 reveals intricate heat transfer characteristics during the impact event. The temperature of the central region of the droplet remains the highest within the simulation domain during the impact. Based on the temperature gradient, the droplet experiences cooling from both the frigid air and the chilly solid surface. Nevertheless, the rate of heat transfer varies. As shown in these illustrations, the highest temperature gradient is observed at the interface between the droplet and the solid substrate, indicating that the droplet is primarily cooled by the surface through conduction. Additionally, the temperature gradient between the droplet and the surrounding cold air is significantly reduced, suggesting that the impact of the cold air is considerably less than that of the surface.

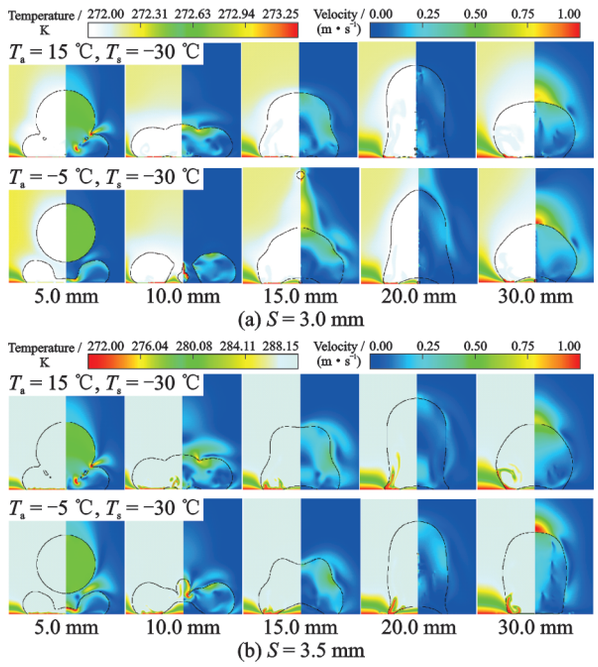

Fig.13 Temperature and velocity evolution of double-droplet continuously impacting superhydrophobic cold surface

2.4 Influence of impact velocity and supercooled degree on result of double-droplet impact

In this section, we aimed to explore the adhesion and rebound characteristics of double-droplet impact on superhydrophobic cold surfaces. Additionally, we compared these findings to the icing and anti-icing behavior observed in the multi-droplet continuous impact-freezing process on superhydrophobic surfaces. To achieve this, we conducted simulations of droplet impacts, varying the velocities and supercooling degrees for comprehensive analysis. Table 2 presents the simulation parameters for droplet impact on superhydrophobic cold surfaces at varying velocities.

Table 2 Simulation conditions of droplets impact superhydrophobic cold surfaces with different velocities

Droplet diameter D_0/mm	Droplet initial velocity V_0/(m•s^{-1})	Air temperature T_a/℃	Surface temperature T_s/℃	Droplet temperature T_0/℃	Droplet spacing S/mm
2.5	0.5, 0.75, 1, 1.25, 1.5, 1.75, 2	−5	−10/−20/−30	0.1	3.0/3.5

Fig.14 illustrates three typical impact results when a cold superhydrophobic surface is continuously impacted by double-droplet: Full adhesion, partial rebound, and full rebound. When heat transfer between cold superhydrophobic surfaces dominates, the contact line freezing rate increases as the surface temperature decreases. This results in an augmented dissipation of droplet viscosity, causing polymerized droplets to lack sufficient energy to detach from the frigid superhydrophobic surface, ultimately leading to full adhesion. Partial rebound takes place when the internal fluid flow resulting from droplet merging is significant, leading to a modification in the velocity vector within the droplets. This causes the merged droplets to resemble a single droplet, with a portion of the fluid becoming detached from the neck. Full rebound occurs when the temperature of the surface is sufficiently low, and the internal fluid flow resulting from contact polymerization assumes the predominant role, leading to detachment of the polymerized droplet from the frigid superhydrophobic surface.

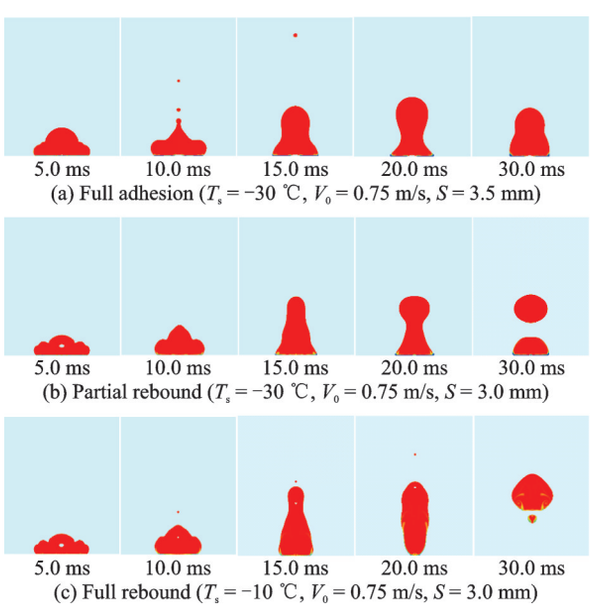

Fig.14 Typical impact results when a cold superhydrophobic surface is continuously impacted by double-droplet

Fig.15 displays the simulation results for different surface temperatures and velocities. For instance, when the surface temperature is −10 ℃, the merged droplet resulting from the impact of the double-droplet on the superhydrophobic cold surface exhibits a higher tendency to rebound. When the surface temperature drops to −20 ℃, under the low impact velocity condition of V_0=0.5 m/s, the combined droplet possesses sufficient energy to detach the ice layer adhering to the bottom and achieve complete rebound. The higher rebound tendency observed in the merged droplet on the superhydrophobic cold surface at −10 ℃ is attributed to the decreased viscous dissipation during the droplet merging process. However, when the impact velocity exceeds 0.75 m/s, the merged droplet loses its ability to generate sufficient force to rupture the ice layer at

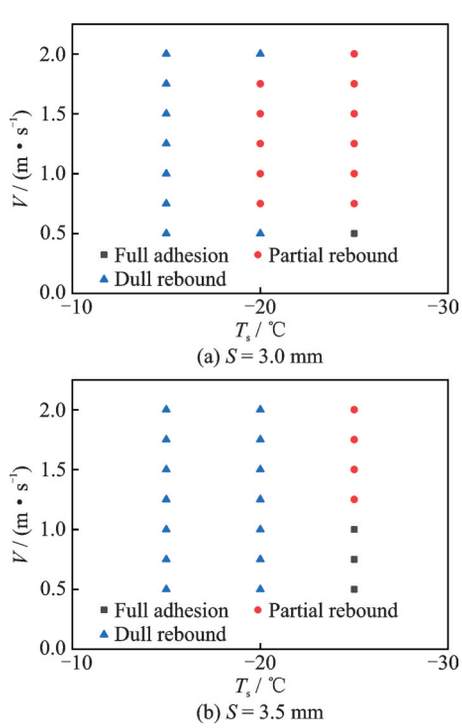

Fig.15 Simulation results of double-droplet impacting cold superhydrophobic surface with different surface temperatures and velocities

the base due to its larger spreading diameter during expansion. As a result, it breaks up from the surface, leaving a portion of the droplet still on the surface. Upon further increase in impact velocity, a noticeable disparity in the inter-droplet distance becomes apparent. In particular, when S=3.0 mm, the double droplet exhibits a fully rebounded form following contact polymerization. For S=3.5 mm, partial rebound is observed after contact polymerization. In this instance, the droplets amalgamate during the contraction phase of the initial droplet. The dissipation of energy is more pronounced, and the amalgamated droplets lack sufficient energy to rupture the ice layer that is attached to the base. When the surface temperature drops to −30 ℃, the double-droplet exhibit a full rebound morphology at low impact velocity V_0=0.5 m/s due to the predominant influence of heat transfer on the cold superhydrophobic surface. However, under all other impact velocity conditions, a partial rebound morphology will occur, and the upper fluid experience an elongated crown height during the tearing process. There are several possible explanations for this outcome: Firstly, the merging of droplets can have a significant impact on the internal fluid dynamics of larger droplets when they collide at high velocities. Consequently, the merged droplets could possess higher internal energy, thereby contributing to their rebound behavior. Additionally, the merging of droplets results in increased droplet size and elongation of the droplet crown height during the rebound process, which is influenced by surface tension.

The findings suggest an interconnection between rebound and adhesion, which arises from the competition between internal fluid dynamics and thermal dissipation on frigid superhydrophobic surfaces due to droplet coalescence. Hence, in the case of successive collisions among numerous droplets, the elevated surface temperature and increased impact velocity are likely to induce the rebound of multiple droplets. This suggests that the superhydrophobic surface retains effective resistance to ice formation during the impact-freezing process of numerous droplets repeatedly colliding with a cold superhydrophobic surface.

3 Conclusions

This paper utilizes numerical simulation techniques to study the freezing behavior of double droplets upon impact on cold surfaces with varying wettability conditions. The research analyzes the influence of surface hydrophobicity, droplet spacing, surface temperature, and initial droplet temperature on the morphological evolution of the double droplets, the spreading coefficient, and the impact outcome. The results reveal the significant impact of droplet coalescence on droplet morphology and fluid dynamics within larger droplets, resulting in enhanced rebound on superhydrophobic surfaces. These findings contribute to a comprehensive understanding of the collision mechanism in continuous collisions of multiple droplets. The following conclusions can be drawn based on the simulation results:

(1) At low impact velocities, the spacing between droplets has a minor effect on hydrophilic surfaces, but it exerts a more significant influence on hydrophobic and superhydrophobic surfaces. The contact process between droplets can be divided into two distinct phases: Spreading and contraction contacts. In the contraction contact phase, the droplets tend to entrain air at the bottom, leading to a reduced contact area between the droplets and the cold surface.

(2) When continuously impacting the hydrophilic surface, the double-droplet shows a 26%—38% increase in the maximum spreading factor for spreading contacts and a 15%—30% increase for contraction contacts, compared to a droplet impact. The superhydrophobic surface shows minimal differences in the maximal spreading coefficients between single and double droplet impact, with variances below 2%.

(3) When double-droplet continuously impact a superhydrophobic cold surface, three typical results are observed: Full rebound, partial rebound, and full adhesion.

These findings demonstrate the complex relationship between droplet coalescence and solidification in the impact-freezing process of double droplets.

References

[1] NEINHUIS C, BARTHLOTT W. Characterization and distribution of water-repellent, self-cleaning plant Surfaces[J].Annals of Botany, 1997,79(6): 667-677.

[2] LIU Xin, ZHANG Xuan, MIN Jingchun. Spreading of droplets impacting different wettable surfaces at a Weber number close to zero[J]. Chemical Engineering Science, 2019, 207: 495-503.

[3] SUN J, LIU Q, LIANG Y, et al. Three-dimensional VOF simulation of droplet impacting on a superhydrophobic surface[J]. Bio-design and Manufacturing, 2019, 2(1): 10-23.

[4] YANG G, GUO K, LI N. Freezing mechanism of supercooled water droplet impinging on metal surfaces [J]. International Journal of Refrigeration, 2011, 34 (8): 2007-2017.

[5] ZHANG R, HAO P F, ZHANG X W, et al. Supercooled water droplet impact on superhydrophobic surfaces with various roughness and temperature[J]. International Journal of Heat and Mass Transfer, 2018, 122: 395-402.

[6] ZHANG H F, ZHAO Y G, LV R, et al. Freezing of sessile water droplet for various contact angles[J]. International Journal of Thermal Sciences, 2016, 101: 59-67.

[7] HUANG L, LIU Z L, LIU Y M, et al. Effect of contact angle on water droplet freezing process on a cold flat surface[J]. Experimental Thermal and Fluid Science, 2012, 40: 74-80.

[8] BLAKE J, THOMPSON D, RAPS D, et al. Simulating the freezing of supercooled water droplets impacting a cooled substrate[J]. AIAA Journal, 2015, 53(7): 1725-1739.

[9] CHANG S N, DING L, SONG M J, et al. Numerical investigation on impingement dynamics and freezing performance of micrometer-sized water droplet on dry flat surface in supercooled environment[J]. International Journal of Multiphase Flow, 2019, 118: 150-164.

[10] ZHANG X, LIU X, WU X M, et al. Impacting-freezing dynamics of a supercooled water droplet on a cold surface: Rebound and adhesion[J]. International Journal of Heat and Mass Transfer, 2020,158: 119997.

[11] XIE F F, LIU G, WANG B B. Coalescence-induced jumping of two unequal-sized nanodroplets[J]. Langmuir, 2018, 34(8): 2734-2740.

[12] BOREYKO J B, CHEN C. Self-propelled dropwise condensate on superhydrophobic surfaces[J]. Physical Review Letters, 2009, 103(18): 184501.

[13] WANG L, XU C Y. Effect of contact angle hysteresis on droplet behaviors: Two-phase lattice Boltzmann simulation[J]. Transactions of Nanjing University of Aeronautics and Astronautics,2013, 30(3): 270-275.

[14] GAO S R, JIN J X, WEI B J, et al. Dynamic behaviors of two droplets impacting an inclined superhydrophobic substrate[J]. Colloids and Surfaces A: Physicochemical and engineering Aspects, 2021, 623: 126725.

[15] WANG X, LIN D J, WANG Y B, et al. Rebound dynamics of two droplets simultaneously impacting a flat superhydrophobic surface[J]. AIChE Journal, 2020, 66(9): 16647.

[16] MA Q, WANG Y F, WANG Y B, et al. Ring-bouncing induced by the head-on impact of two nanodroplets on superhydrophobic surfaces[J]. Physics of Fluids, 2023, 35(4): 042013.

[17] WANG Y F, WANG Y B, ZHANG C Z, et al. Retraction and bouncing dynamics of nanodroplets upon impact on superhydrophobic surfaces[J]. Physics of Fluids, 2023, 35 (3): 032012.

[18] ANSYS Inc. ANSYS fluent theory guide[M]. Release 2020 R2. Canonsburg, PA, USA: ANSYS, Inc., 2020.

[19] HIRT C W, NICHOLS B D. Volume of fluid (VOF) method for the dynamics of free boundaries[J]. Journal of Computational Physics, 1981, 39 (1): 201-225.

[20] BRACKBILL J, KOTHE D, ZEMACH C. A continuum method for modeling surface tension[J]. Journal of Computational Physics, 1992,100: 335-354.

[21] HOU J Q, GONG J Y, WU X, et al. Numerical study on impacting-freezing process of the droplet on a lateral moving cold superhydrophobic surface[J]. International Journal of Heat and Mass Transfer, 2022, 183: 122044.

[22] LIU X, MIN J C, ZHANG X, et al. Supercooled water droplet impacting-freezing behaviors on cold superhydrophobic spheres[J]. International Journal of Multiphase Flow, 2021,141: 103675.

Acknowledgement This work was supported by the Open Fund of Key Laboratory of Icing and Anti/De-icing (No. IADL20190311).

Author Dr. **HU Anjie** received the B.S. degree in thermal energy and power engineering and Ph.D. degree in engineering thermophysics from Chongqing University, Chongqing, China, in 2010 and 2015, respectively. From 2015 to present, he has been with the School of Civil Engineering and Architecture, Southwest University of Science and Technology, where he is currently a full associate professor. His research has focused on gas-liquid two-phase flow and heat transfer simulation, which includes bubble growth in boiling heat transfer, droplet splash dynamics, icing of droplets.

Author contributions Dr. **HU Anjie** designed the study, complied the models, interpreted the results and revised the manuscript. Mr. **YUAN Qiaowei** conducted the analysis, interpreted the results and wrote the draft of the manuscript. Ms. **GUO Kaiyue** contributed to data and model components for the numerical model. Dr. **LIU Dong** contributed to the discussion and background of the study. All authors commented on the manuscript draft and approved the submission.

Competing interests The authors declare no competing interests.

(Production Editor: SUN Jing)

双液滴对不同润湿性冷表面连续撞击的数值模拟

胡安杰，袁侨伟，郭凯月，刘　东

(西南科技大学土木工程与建筑学院，绵阳 621010，中国)

摘要：采用凝固/熔化模型和VOF(Volume-of-fluid)模型相结合的数值模拟方法研究了双液滴在低速条件下以不同的润湿性连续冲击冷表面的冻结行为。对比了液滴两种接触模式(扩散接触和收缩接触)下的液滴铺展及相变过程。模拟结果表明，液滴的聚结对液滴的形态有显著影响。当双液滴连续冲击亲水表面时，扩散接触的最大扩散因子相比单液滴增加26%～38%，收缩接触的最大扩散因子比单个液滴冲击增加15%～30%。而在超疏水表面上，单、双液滴冲击之间的最大扩散系数差异小于2%，可以忽略不计。此外，对双液滴在低温下与超疏水表面发生碰撞进行分析，得到完全反弹、部分反弹和完全粘附3种撞击结果在不同接触模式下液滴聚合以及凝固过程的影响规律。

关键词：双液滴；结冰；凝固融化模型；VOF模型；超疏水表面